ResearchGate

See discussions, stats, and author profiles for this publication at: https://www.researchgate.net/publication/342240982

Pink Axinite from Merelani, Tanzania: Origin of Colour and Luminescence

Article *in* The Journal of Gemmology · June 2020

DOI: 10.15506/JoG.2020.37.2.192

CITATIONS
0

READS
750

2 authors:

Maxence Vigier
Institut des Materiaux Jean Rouxel
10 PUBLICATIONS **4** CITATIONS
SEE PROFILE

E. Fritsch
Institut des Materiaux Jean Rouxel
144 PUBLICATIONS **1,504** CITATIONS
SEE PROFILE

All content following this page was uploaded by Maxence Vigier on 26 September 2020.

The user has requested enhancement of the downloaded file.

Pink Axinite from Merelani, Tanzania: Origin of Colour and Luminescence

Maxence Vigier and Emmanuel Fritsch

ABSTRACT: Two pink axinites from Merelani, Tanzania, were characterised with standard gemmological techniques, energy-dispersive spectroscopy, and UV-Vis-NIR, Raman and luminescence spectroscopy. We compared them to three other samples from Merelani (pinkish orange, blue and near-colourless) and one brown axinite from Oisans, France. Chemical analysis revealed that the two pink axinites correspond to axinite-(Mg). UV-Vis-NIR spectroscopy revealed that the origin of the pink colouration is a large, asymmetric broad band centred at about 560 nm. Its position and shape are typical for Mn^{3+}. Manganese is also present in both samples as Mn^{2+}, and we surmise that natural radiation from nearby minerals converted some Mn^{2+} into Mn^{3+}. The orange luminescence of the axinites (weaker under short-wave UV radiation) is related to a broad emission band at 631 nm caused by Mn^{2+}, and a more unusual red luminescence is associated with features at 688 and 694 nm attributed to Cr^{3+}. Raman spectroscopy showed slight variations between the different axinite species, but further research is needed to associate each axinite end member with its characteristic Raman spectrum.

The Journal of Gemmology, **37**(2), 2020, pp. 192–205, https://doi.org/10.15506/JoG.2020.37.2.192
© 2020 Gem-A (The Gemmological Association of Great Britain)

Axinites are rarely encountered collector's stones that are most commonly brown, but may display attractive blue, yellow to orange, and (rarely) pink to purple colouration. Despite having sufficient hardness (Mohs 6–7), axinite is seldom found mounted in jewellery.

Axinite is the name of a borosilicate mineral group containing four different species (Burke 2008), and three of them have been found in gem quality:

- Axinite-(Fe): $Ca_4Fe^{2+}_2Al_4[B_2Si_8O_{30}](OH)_2$, formerly called ferro-axinite (the most common axinite species)
- Axinite-(Mg): $Ca_4Mg^{2+}_2Al_4[B_2Si_8O_{30}](OH)_2$, formerly called magnesio-axinite (e.g. Figure 1)
- Axinite-(Mn): $Ca_4Mn^{2+}_2Al_4[B_2Si_8O_{30}](OH)_2$, formerly called manganaxinite

A distinctive component of the axinite structure, which has triclinic symmetry, is the $B_2Si_8O_{30}$ group, in the centre of which two isolated BO_4 tetrahedra and two Si_2O_7 groups constitute a six-membered ring, while the other cations occupy sites in octahedral coordination with oxygen.

Axinite Colours

Both Fe^{2+} and Mn^{2+} are potentially colour-inducing ions. Nevertheless, axinite-(Mn) can be nearly colourless (Lauf 2007; see also www.mindat.org/min-1459.html) because Mn^{2+} is a poor absorber of visible light. However, when Mn^{2+} is present in a larger atomic proportion than in the axinite structure (e.g. in rhodochrosite, $MnCO_3$), then this ion can induce colour. All iron-containing axinites (whatever the species) are brown (Faye 1972; Pohl *et al.* 1982; Wilson *et al.* 2009; see also www.mindat.org/min-1459.html). Axinite-(Mg) does not contain any colour-causing cation in its nominal chemical composition, and is thus intrinsically colourless. However, it commonly shows various colours including yellowish orange, brown to pink and purple to blue (Quinn & Breeding 2005; Wilson *et al.* 2009; Pay 2017; see also Figure 1), which are probably due to different minor- and

Figure 1: Axinite from Merelani, Tanzania, can show various colours (top), and some of the samples depicted here exhibit strong reddish orange fluorescence to long-wave UV radiation (bottom). Based on their colouration and origin, all of these stones are most likely axinite-(Mg). The largest faceted gem weighs 4.22 ct. Courtesy of Bill and Elke Vance, Vance Gems; photos by Jeff Scovil.

trace-element impurities. The fourth member of the axinite group, tinzenite—ideally $Ca_2Mn^{2+}_4Al_4[B_2Si_8O_{30}](OH)_2$—contains less than 3 Ca per formula unit due to substitution of Ca^{2+} by Mn^{2+}. It appears to be intrinsically yellow to orange (depending on sample thickness), and this colour is presumably induced by Mn^{2+}, which in some cases may colour minerals orange (as in serandite or spessartine).

'Blue' axinite is known to contain vanadium (Jobbins *et al.* 1975), which Schmetzer (1982) related to the blue colouration for the first time, with an absorption band near 575 nm. More recent work clearly demonstrates that blue axinite is coloured by V^{3+} (Arlabosse *et al.* 2008), which induces a broad band at about 592 or 597 nm (Williams *et al.* 2014). This feature causes transmission in the blue region when viewed perpendicular to the flat Tanzanian crystals. A similar absorption feature has been documented in axinite-(Mg) from Merelani, Tanzania (http://minerals.gps.caltech.edu/FILES/Visible/Axinite/Index.html). The exact position of the absorption maximum depends on crystal orientation (axinite is biaxial), but overall the colour appears blue to blue-violet. Fritz *et al.* (2007) noted that blue zones in axinite-(Fe) from Pakistan showed an absorption maximum in the 580 nm range, but they did not analyse for vanadium.

A noticeable colour change is sometimes encountered in axinite (e.g. Lauf 2007; Williams *et al.* 2014), appearing blue-grey in fluorescent light or daylight, and purple in incandescent light. To date, this effect has been noticed only in some axinite-(Mg) and axinite-(Mn) specimens from Tanzania.

Axinite Pleochroism and Optic Character

Axinite is commonly described as being pleochroic (Gribble & Hall 1992; Association Française de Gemmologie 2013; see also http://webmineral.com/data/Axinite-(Mg).shtml). Pleochroism in Tanzanian axinite was mentioned for the first time by Jobbins *et al.* (1975). The pleochroism ranged from pale blue to violet to grey, and similar colouration was also noted decades later in various Tanzanian axinites (Jang-Green *et al.* 2007; Arlabosse *et al.* 2008; Williams *et al.* 2014), as well as pale yellow to green pleochroism (Milton *et al.* 1953).

Mineralogy textbooks mention axinite as being biaxial positive or negative. However, the optic character is rarely mentioned in gemmological journals. Jobbins *et al.* (1975) observed that Tanzanian axinite is biaxial positive in contrast to most axinites, which are biaxial negative. The book *Gemmes* (Association Française de Gemmologie 2013) indicates that axinite is biaxial negative, except for axinite-(Mg).

Axinite Luminescence

The fluorescence of axinite-(Mg) from Tanzania has been described as a distinct orange-red to long-wave UV radiation (365 nm) and a duller red under short-wave UV (254 nm; Jobbins *et al.* 1975). Similar descriptions of the luminescence for axinite-(Mg) or axinite-(Mn) are noted in the literature (Jang-Green *et al.* 2007; Lauf 2007; Arlabosse *et al.* 2008; Jaszczak & Trinchillo 2013; Pay 2017). By contrast, axinite-(Fe) is inert, which is not surprising since Fe often quenches luminescence (Fritsch & Waychunas 1994).

This Study

The present study investigates the origin of colour and luminescence in two dominantly pale pink axinites from Merelani, Tanzania, and compares their properties to those of axinite showing other colours. In addition to the two gems of interest, three of the other samples also came from Merelani, which has produced both axinite-(Mg) and axinite-(Mn) in gem quality.

Merelani is a famous mineral deposit located in northeast Tanzania, and is best known for its tanzanite and tsavorite (e.g. Wilson *et al.* 2009). The deposit occurs in the Neoproterozoic Mozambique Belt, an area with an extensive geologic history and hosting a variety of gem and mineral deposits (Malisa & Muhongo 1990; Malisa 2003, 2005; Olivier 2006; Feneyrol 2012; Harris *et al.* 2014). The Merelani area is underlain by metacarbonate and metasilicate rocks such as marble and graphite-bearing gneiss, which were affected by greenschist-facies retrograde metamorphism. The axinite there is commonly associated with an assemblage consisting of zoisite (tanzanite), grossular (tsavorite), tremolite, diopside, K-feldspar, muscovite, chlorite, prehnite and zircon.

MATERIALS AND METHODS

The six axinites studied for this report are listed in Table I. The two rare pink axinite cabochons (samples 2999 and 3000) were obtained through Dudley Blauwet. For comparison, two axinite crystals from Merelani (3356 and 3357) were acquired from Joyce van Dronkelaar-Kessy, and a faceted axinite (3355) from this locality was provided by Denis Gravier. In addition, we included a brown axinite (2290a) from Oisans, France, from the personal collection of author EF. All samples were studied in the form that they were originally received except for sample 2290a, which was polished to obtain two parallel windows.

Standard gemmological measurements were recorded for all six samples. RI and optic sign were obtained using an A. Krüss Optronic ER604 refractometer (resolution of 0.01).

Table I: Characteristics of the six axinite samples.

Sample no.	Locality	Dimensions (mm)	Weight (g)	Sample type	Colour	Photo*
2290a	Oisans, France	10.4 × 8.3 × 2.5	0.48	Parallel-polished rough	Brown	
2999	Merelani, Tanzania	19.8 × 6.0 × 4.8	1.11 (5.55 ct)	Cabochon	Bicoloured purplish pink and orangey pink; weak cat's eye	
3000	Merelani, Tanzania	19.2 × 10.6 × 3.4	1.18 (5.90 ct)	Cabochon	Pink	
3355	Merelani, Tanzania	4.5 × 3.7 × 2.5	0.06 (0.30 ct)	Rectangular cushion	Pinkish orange	
3356	Merelani, Tanzania	26.5 × 22.3 × 2.7	4.09	Flat crystal	Blue	
3357	Merelani, Tanzania	26.0 × 14.7 × 4.9	3.29	Flat crystal	Near-colourless	

* Photos by M. Vigier (2290a, 3000, 3356 and 3357) and Orasa Weldon (2999 and 3355).

Hydrostatic SG was measured with a Mettler-Toledo XS104 balance, using a semi-automated system. Reaction to UV radiation was observed with a Vilber-Lourmat VL-215.LC UV lamp, which includes two 15 W UV tubes (long- and short-wave) that are approximately 30 cm long. Observations were done at a fixed distance of 7 cm from the lamp, in a darkened room, against an inert black background. Internal features and pleochroism were observed with a Leica MZ6 binocular microscope with Nossigem gemmological observation attachments, including polarising filters.

Quantitative chemical analyses were obtained for all samples with a JEOL 5800 LV scanning electron microscope (SEM) equipped with a Princeton Gamma Tech (PGT) energy-dispersive spectrometer (EDS). The instrument featured an IMIX-PTS detector, which includes a 'high-resolution' (115 eV) Ge crystal and an ultra-thin polymer window that, under ideal conditions, can be used to detect elements as light as boron (if present as a major component of the material). The SEM was operated using a beam accelerating potential of 15 kV and a 0.5 nA current, with a 37° take-off angle to the detector. The working distance between the bottom of the column and the sample surface was 15 mm. Standards used were either pure elements or simple compounds. The data were processed using PGT software incorporating a Phi-Rho-Z correction. Oxygen was calculated from the EDS spectrum instead of from stoichiometry. Analytical

precision is estimated at 1–2% for samples that have a perfectly polished, flat surface perpendicular to the beam, which was not the case for most of the stones in this study.

Raman spectroscopy was performed on all samples with a Bruker MultiRAM Fourier-transform Raman spectrometer, equipped with an Nd:YAG laser at 1064 nm. The laser power was nominally 300 mW and the resolution was 4 cm^{-1}. Fifty spectra were accumulated per measurement. To obtain a better-quality Raman spectrum of sample 2290a, we used a Horiba Jobin Yvon T64000 dispersive Raman spectrometer equipped with a 514 nm Ar^{+} laser (resolution of 4 cm^{-1}).

Ultraviolet-visible-near infrared (UV-Vis-NIR) absorption spectra were collected from all samples with a Magilabs GemmoSphere spectrometer, in the spectral range of 365–1000 nm with a sampling interval of 1.3 nm; only results for the approximately visible range are given in this article. The sample was placed at the bottom centre of an integrating sphere. This setup does not impose the rectilinear pathway of light from lamp to detector (as in standard spectrometers), and thus it analyses all light going through the sample. In addition, any potential luminescence that was excited by visible light in the gem was collected by the instrumentation.

Photoluminescence emission and excitation spectra were obtained for all samples using a Fluorolog-3 instrument from Horiba Jobin Yvon in conjunction with FluorEssence software. A Synapse CCD detector was coupled with an iHR320 spectrometer. Both excitation and emission measurements had a resolution down to 1 nm; enhanced resolution below 1 nm was obtained by juxtaposing several scans to cover a given spectral domain in several sections.

RESULTS

Standard Gemmological Data

The results of RI, optic character and SG measurements are presented in Table II. Because of the difficulties imposed by the shape or surface conditions of the samples, only average RI values (i.e. of the lowest and highest measurements) are reported. However, RI data are not reported for sample 2999 because it was not possible to obtain consistent measurements due to its shape and polish. The optic character of most of our samples was biaxial negative, except for two biaxial positive samples (both of which were axinite-(Mg), as specified below).

All of the axinites displayed pleochroism when observed with polarisers. For thin or pale samples, colour perception was enhanced by looking down the long direction of the crystals (i.e. longer optical path length). The pleochroic colours are shown in Figure 2 and summarised as follows:

- 2290a and 3356: blue, purple and brown (e.g. Figure 2a)
- 2999 and 3000: pale blue, pink and nearly colourless (e.g. Figure 2b)
- 3355 and 3357: pale blue, purple and yellow (e.g. Figure 2c)

In summary, the pleochroic colours are rather similar from one sample to another, varying mostly in intensity.

UV fluorescence reactions of our samples are described in Table II and illustrated in Figure 3. With the exception

Table II: Standard gemmological properties of the six axinites.

Sample no.	Average RI	Optic character*	SG	UV luminescence	
				Short-wave	Long-wave
2290a	1.68	B–	3.24	Inert	Inert
2999	—	—	3.19	Weak orange-red	Intense orange
3000	1.66	B+	3.15	Weak orange-red	Intense orange
3355	1.68	B+	3.10	Weak orange-red	Intense orange
3356	1.67	B–	3.20	Weak orange-red	Intense orange
3357	1.67	B–	3.21	Very weak purple	Moderate orange and purple

*Abbreviations: B– = biaxial negative, B+ = biaxial positive.

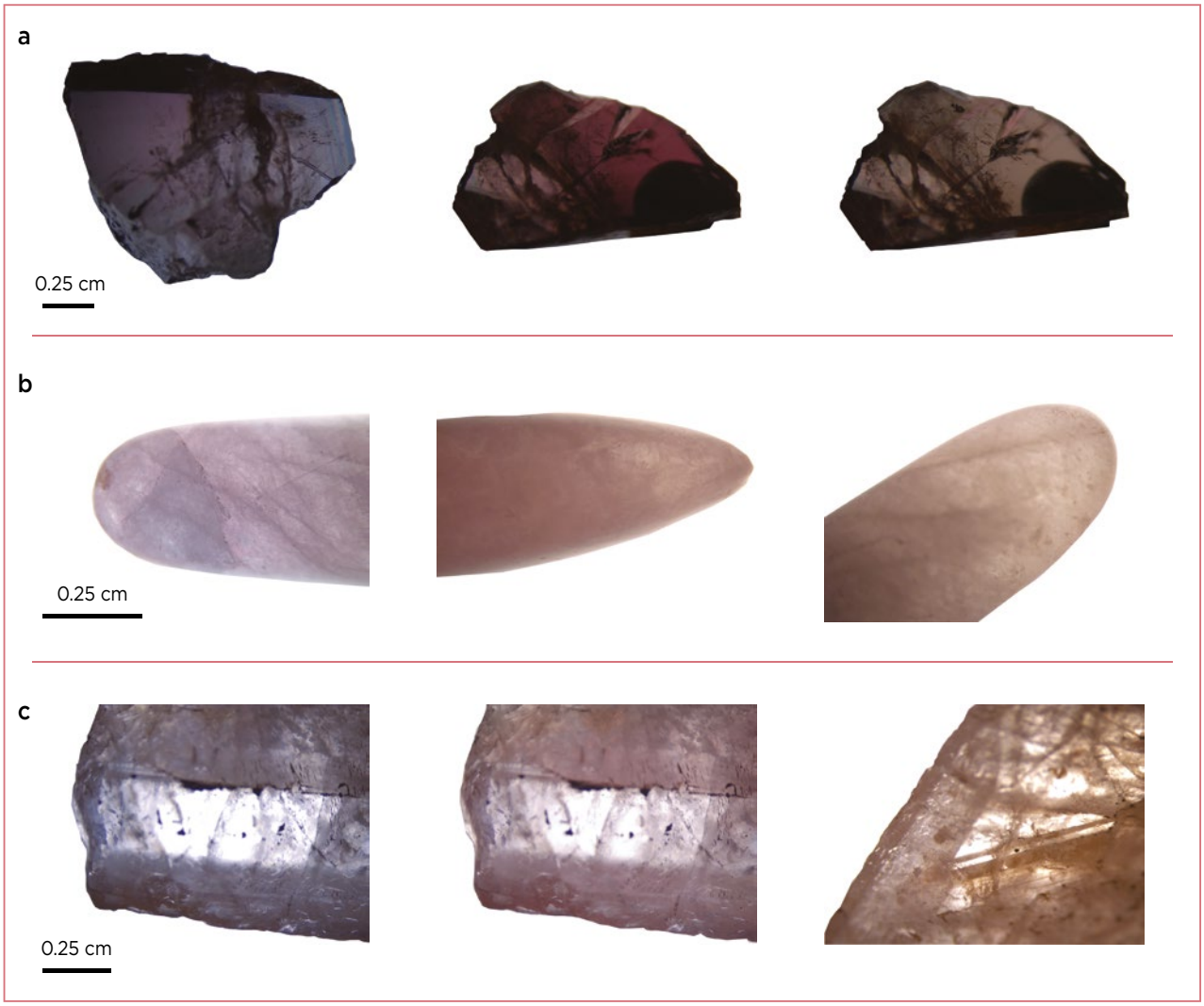

Figure 2: Pleochroism (here described in each photo from left to right) is shown for three representative samples from this study: (**a**) axinite-(Fe) sample 2290a, in blue, purple and brown; (**b**) axinite-(Mg) sample 2999, in pale blue, pink and nearly colourless; and (**c**) axinite-(Mn) sample 3357, in pale blue, purple and yellow. Photomicrographs by M. Vigier.

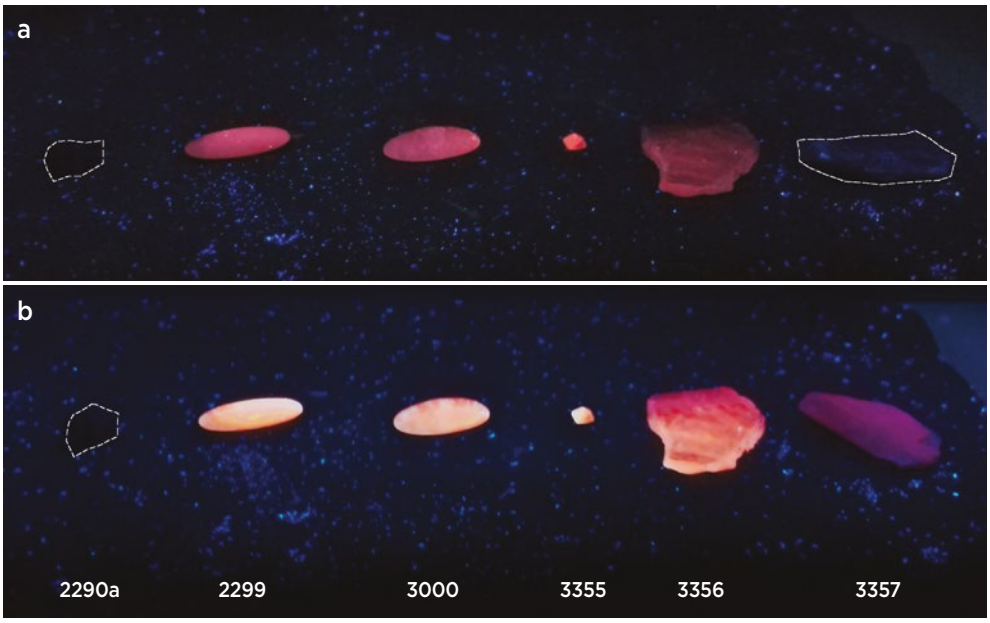

Figure 3: The six axinite samples are shown here in (**a**) short-wave and (**b**) long-wave UV radiation. Those showing very weak or no fluorescence are outlined. See Table I for sample weights. Photos by M. Vigier.

Figure 4: Axinite-(Mg) sample 2999 displays a weak cat's-eye effect, as well as colouration that ranges from orangey pink to purplish pink. The stone weighs 5.55 ct and is cut as a double cabochon. Photo by Orasa Weldon.

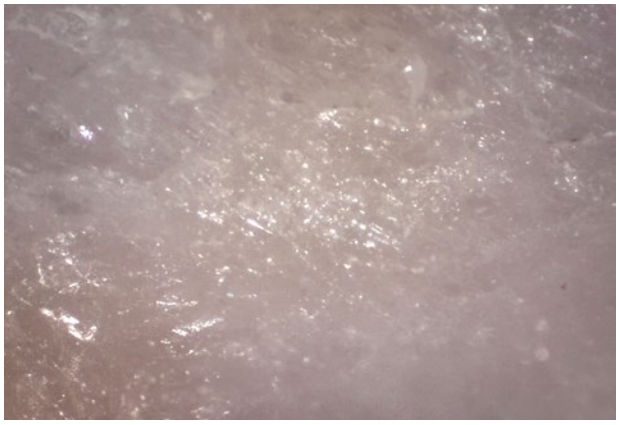

Figure 5: The cabochon in Figure 4 contains numerous tiny reflective fractures in a fairly consistent orientation that are responsible for its weak chatoyancy. Photomicrograph by Brendan M. Laurs; image width 1.0 mm.

of the brown sample (which was inert), the gems emitted mostly orange fluorescence, sometimes with a touch of red. The emission was weaker to short-wave UV, as is the case for the luminescence of many gems. For sample 3356, the crystal termination showed distinctly redder fluorescence than the rest of the stone. Sample 3357 displayed a weak purple luminescence.

Sample 2999 was bicoloured (purplish pink and orangey pink) and also showed weak chatoyancy, as illustrated in Figure 4. Magnification revealed that the cat's-eye effect was caused by reflections (sometimes iridescent) from many small, parallel fractures (possibly cleavages; Figure 5). The somewhat indistinct cat's-eye was directionally aligned along the length of the stone, indicating that the cabochon's elongate high-domed shape mainly controlled the distribution of the chatoyancy. The gem also contained a number of partially healed fissures consisting of fluid inclusions.

Chemical Composition

As axinite is a mineral group, it was desirable to determine which species of axinite our samples represented. For that purpose, SEM-EDS chemical analyses were compared to our Raman spectroscopy data (see below). Chemical analyses of the six samples are presented in Table III, and comparisons with chemical data taken from the literature for each of the three axinite species are available in the online data depository on *The Journal*'s website.

We looked for V and Cr with our instrumentation but did not detect either element (detection limits were high, at around 0.1% wt.%). Analysis of sample 3000 gave a total of only about 85%, and a carefully executed second round of analyses gave a similar low total, for which we have no explanation.

Two of the specimens approached end-member compositions—axinite-(Mg) sample 3000 and axinite-(Mn) sample 3356—whereas the other four were of intermediate composition (Figure 6). The bicoloured cabochon (2999) and the faceted stone (3355) were found to be axinite-(Mg) with significant Mn contents, whereas sample 3357 was axinite-(Mn). The brown sample 2290a was axinite-(Fe).

Raman Scattering

The Raman spectra of the six axinites were similar in general shape, as expected because of their common structure. Nevertheless, details of the band positions varied slightly according to the specific species (e.g. Figure 7). For example, the peak at 302 cm^{-1} in axinite-(Mg) was found at 308 cm^{-1} in axinite-(Fe), and the feature at 493 cm^{-1} in axinite-(Mg) moved to 486 cm^{-1} in axinite-(Fe). These were reproducible, measurable differences (which could therefore help with species identification). Although crystallographic orientation was not taken into account for these spectra, it would only affect the peak intensities and not peak positions, as is the case for vibrational spectroscopy.

Visible-range Absorption Spectroscopy

The main goal of this investigation was to determine the origin of the pink to purple colour in axinite. Figure 8 compares the absorption spectra obtained from the two pink axinites. The spectra were obtained perpendicular to the base of each cabochon, and not in a specific crystallographic orientation. However, both the peak positions and intensities may change with orientation, as is the case for electronic transitions. Nevertheless, based on the polarised spectra given for axinite-(Mg) from Merelani at http://minerals.caltech.edu/FILES/Visible/Axinite/Index.html, it appears that such changes are rather small.

The pink colouration is related to a broad, asymmetric band with an apparent maximum at about 560 nm

Table III: Chemical composition by SEM-EDS of the six axinite samples.*

Sample	Axinite-(Fe)	Axinite-(Mg)	Axinite-(Mg)	Axinite-(Mg)	Axinite-(Mn)	Axinite-(Mn)
Number	2290a	2999	3000	3355	3356	3357
Colour	Brown	Purplish pink and orangey pink	Pink	Pinkish orange	Blue	Near-colourless
Locality	France	Tanzania	Tanzania	Tanzania	Tanzania	Tanzania
Oxides (wt.%)						
SiO_2	42.34	43.13	39.60	45.47	42.66	41.82
Al_2O_3	17.01	18.01	16.19	18.37	17.33	16.76
FeO	6.94	0.10	0.11	nd	0.08	1.84
MgO	1.56	4.62	6.82	4.36	0.55	2.27
MnO	2.16	4.14	0.19	4.86	10.28	6.00
CaO	19.37	19.97	14.99	21.22	19.32	20.17
B_2O_3 calc	6.02	6.21	5.56	6.49	6.05	6.00
H_2O calc	1.56	1.61	1.44	1.68	1.57	1.55
Total	96.96	97.78	84.90	102.45	97.84	96.41
Cations per 32 (O, OH)						
Si	8.150	8.052	8.256	8.122	8.168	8.082
B	2.000	2.000	2.000	2.000	2.000	2.000
Al	3.858	3.962	3.978	3.866	3.910	3.818
Fe tot	1.118	0.016	0.020	nd	0.012	0.298
Mg	0.448	1.286	2.120	1.160	0.156	0.654
Mn	0.352	0.654	0.034	0.736	1.668	0.982
Ca	3.994	3.994	3.348	4.060	3.964	4.176
OH	2.000	2.000	2.000	2.000	2.000	2.000
Total cations (excluding OH)	19.920	19.966	19.754	19.946	19.878	20.010

*Abbreviation: nd = not detected.

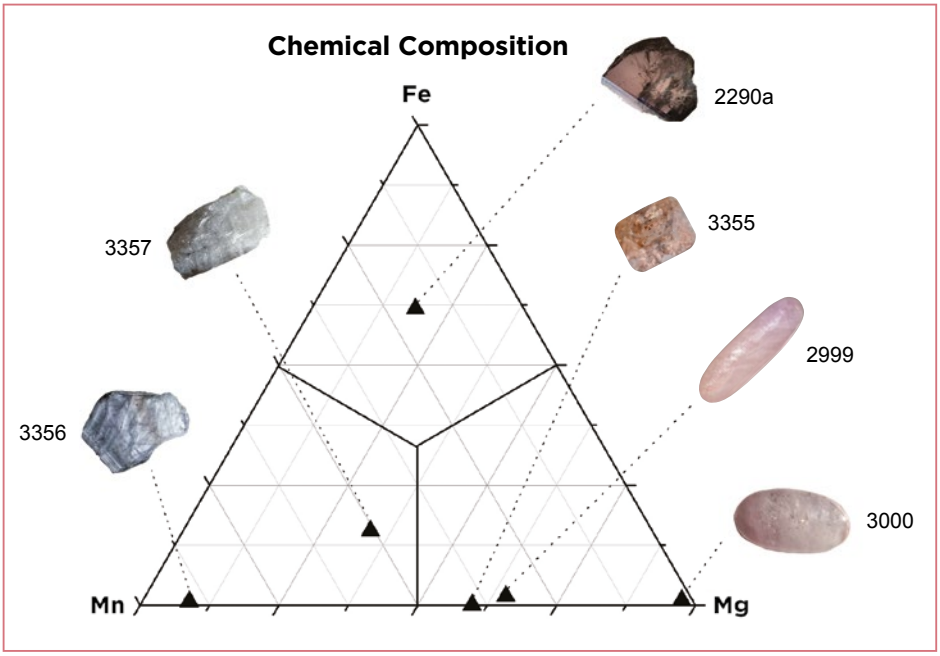

Figure 6: Chemical compositions (molecular proportions) of the six axinite samples are plotted in terms of the three end members axinite-(Fe), axinite-(Mn) and axinite-(Mg).

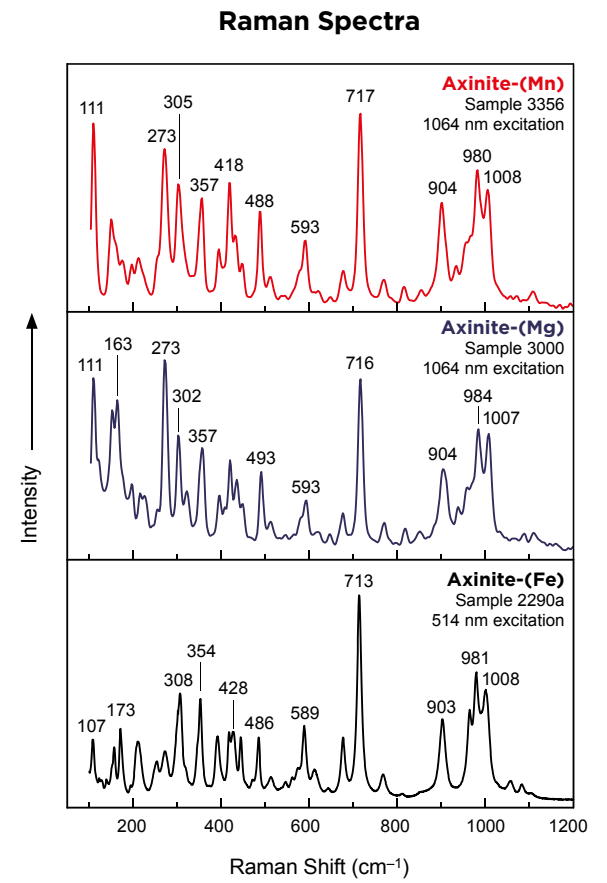

Figure 7: Raman spectra are shown for three samples that are most representative of axinite-(Mn), axinite-(Mg) and axinite-(Fe).

(again, see Figure 8). According to this band position, the 'pink' colour is actually a light purple. The band maximum being positioned higher than 550 nm favours a transmission window in the blue, thus inducing purple rather than pink. In sample 2999, a band at about 508 nm is present as well, absorbing green and blue, thus leading to a yellower hue that shifts the pink colour towards orangey pink. When the 508 nm peak is smaller than the one at 560 nm, purplish pink is seen.

Other features include a sharp peak at 412 nm with a shoulder at about 420 nm. These, and the broad band at 508 nm mentioned above, are well-known Mn^{2+} features, which should be accompanied by two weak, broad bands at higher wavelength, not clearly seen here (Burns 1993). Similar features would be expected to colour yellow to orange tinzenite, which is richer in Mn^{2+}. A small sharp feature recorded at 694 nm—appearing as a negative peak with the type of spectrometer used—is also encountered most notably in ruby. It is likely the result of Cr^{3+} emission (see below).

Figure 9 compares the absorption spectra of the pink axinites to those of the non-pink samples. The well-documented band at about 583 nm (depending on orientation) that is due to V^{3+} induced a pale blue-violet colour component, even though vanadium was below the detection limit of our SEM-EDS instrumentation (consistent with Arlabosse *et al.* 2008, although they detected approximately 0.1 wt.% V_2O_3 using long count times). According

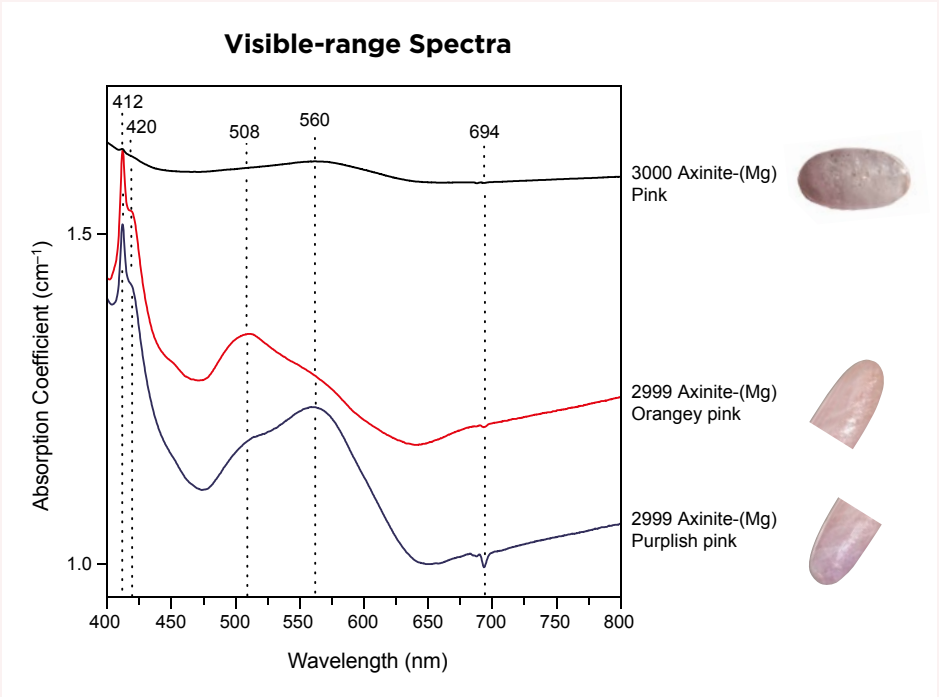

Figure 8: Visible-range absorption spectra are shown for pink axinite sample 3000 and for bicoloured sample 2999 (orangey pink and purplish pink portions). The pink colour is due to a broad, asymmetric band centred at about 560 nm. Other features include a sharp peak at 412 nm with a shoulder at about 420 nm, and a broad band at 508 nm. Spectra are offset vertically for clarity.

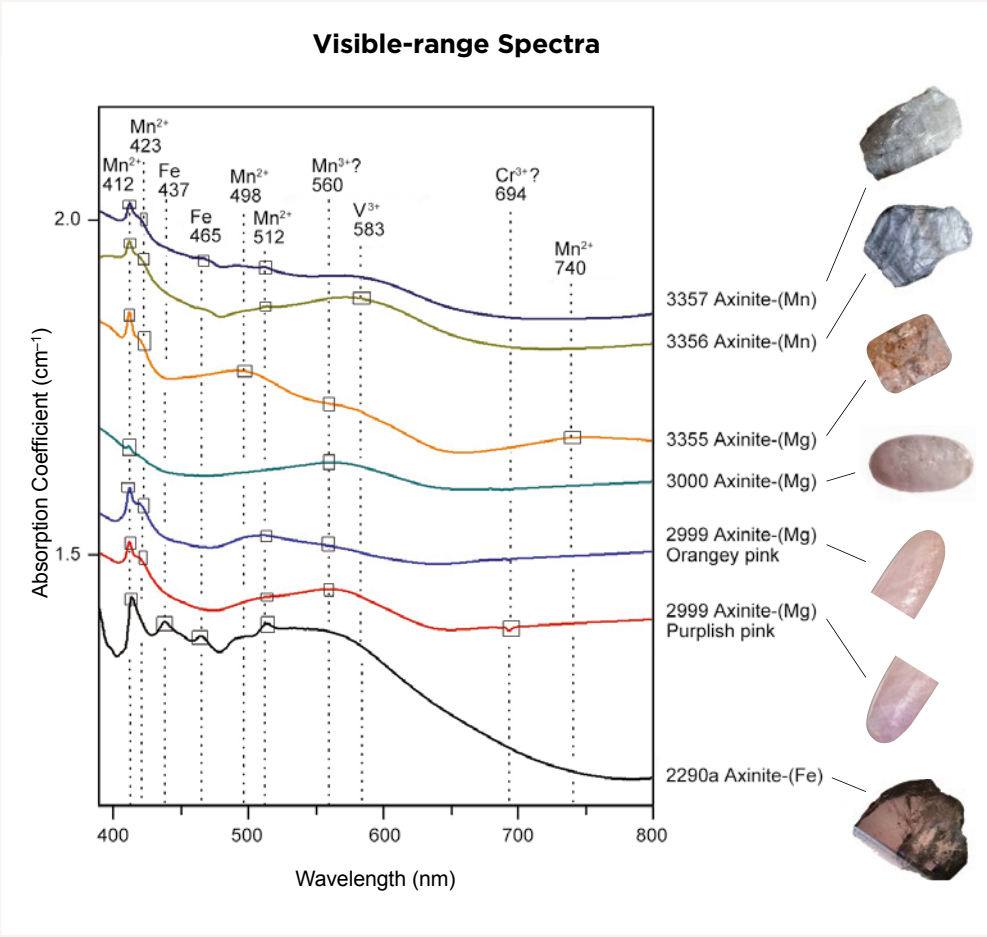

Figure 9: Visible-range absorption spectra are shown for all six axinites studied. The band at about 560 nm appears to cause colour only in the pink samples. Assignments to transition metal ions are also given for the other bands present. Spectra are offset vertically for clarity.

to previous studies, vanadium is not related to pink-to-purple colour in axinite, but rather to blue (Jobbins *et al.* 1975; Schmetzer 1982), as the absorption maximum is located further towards the red region.

Thus, the pink colouration of these axinites is associated with the asymmetric 560 nm band. Such an asymmetric band centred at about 550 nm is a classic feature of Mn^{3+} in many minerals and materials. For example, Mn^{3+} colours pink 'morganite' beryl, purple 'lepidolite' mica and pink-to-red 'rubellite' tourmaline (Reinitz & Rossman 1988; Platonov *et al.* 1989; http://minerals.caltech.edu/FILES/Visible/mica/index.html). In addition, we know there is at least 0.19 wt.% MnO in the two pink axinite gems. Therefore, there is enough manganese to have the small amount of Mn^{3+} necessary to cause the colour, as this ion is a strong light absorber. There are no other transition-element ions present that could cause this kind of absorption feature. As a consequence, the only interpretation consistent with all the data is that Mn^{3+} is responsible for the 560 nm feature, and therefore we propose that this ion is responsible for the pink colour in axinite. The pink to purplish pink is a mixture of red (transmission window above 640 nm) and some blue (transmission window between 450 and 500 nm), whereas in blue axinite the red is nearly fully absorbed.

Photoluminescence Emission and Excitation Spectroscopy

Figure 10 compares emission spectra obtained from two different-luminescing areas (showing typical orange and more reddish fluorescence) of sample 3000 under 365 nm (long-wave UV) excitation. A broad band (slightly less than 100 nm wide) with an apparent maximum at 631 nm is common to both spectra. This band is more intense for the orange-luminescing area. Although 631 nm is at the border between orange and red, the human eye is much more sensitive in the orange region (approximately 590–630 nm) so the perceived colour is a relatively pure orange. Two sharp peaks at 688 and 694 nm in the red region are also present, as expected, in the area of the sample showing more reddish luminescence.

Excitation spectra were then collected from sample 3000 to reveal which wavelengths excite the specific

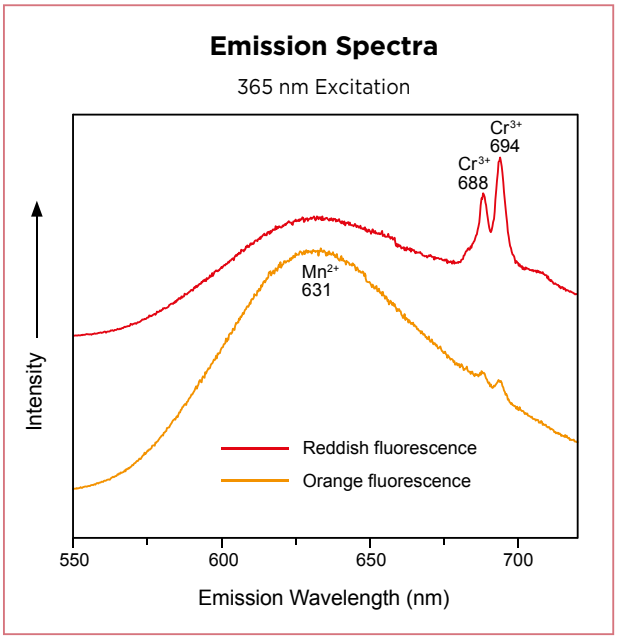

Figure 10: Emission spectra obtained using 365 nm (long-wave UV) excitation from two different areas of sample 3000 demonstrate that the orange luminescence of pink axinite is due to a large band centred at about 631 nm (related to Mn^{2+}) and the reddish fluorescence is caused by the addition of Cr^{3+} features at 688 and 694 nm (top spectrum).

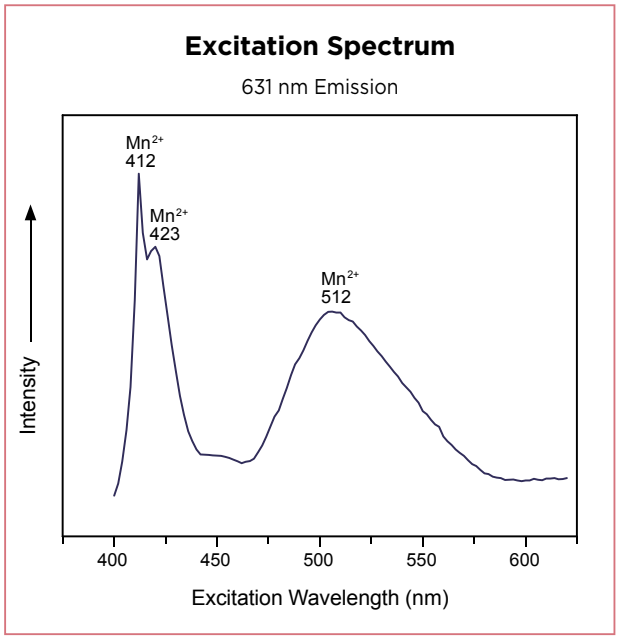

Figure 11: The excitation spectrum of axinite sample 3000 for 631 nm emission shows a close resemblance to the visible-range absorption spectrum of Mn^{2+} (i.e. the orangey pink portion of sample 2999 in Figure 8), which demonstrates that the orange luminescence is due to Mn^{2+}.

emissions at 631 nm (orange) and 694 nm (red). An excitation spectrum reveals which wavelengths excite a specific emission. These wavelengths thus represent the absorption(s) responsible for the emission, and comparing the excitation spectrum with the absorption spectrum in the visible range helps establish the origin of the luminescence. The excitation of the orange emission at 631 nm (Figure 11) is nearly identical in shape to the absorption of Mn^{2+} in the orangey pink portion of sample 2999 (Figure 8). As a consequence, the orange fluorescence of the axinite can be attributed to Mn^{2+}. This ion is well known to be responsible for this luminescence colour in a number of minerals (e.g. apatite, calcite and other carbonates, spodumene and many other silicates; El Ali *et al.* 1993; Robbins 1994). For the excitation of the red emission at 694 nm (Figure 12a), the features include absorption bands of Mn^{2+} as well as a sharp band about 648 nm, along with underlying, broad absorption in the 550–650 nm region. These last two features might be related to Cr^{3+} absorption, and they are indeed present at about the same positions in the excitation spectrum of ruby (Figure 12b), in which they are known to be due to emission from pairs of chromium ions, that is Cr^{3+}–Cr^{3+} (Robbins 1994; Gaft *et al.* 2005). In addition, the emission doublet (i.e. at 658 and 668 nm in the ruby spectrum) is quite characteristic of Cr^{3+} and has been documented in a number of minerals (Gaft *et al.* 2005). Thus, we surmise that the reddish component of axinite luminescence is due to Cr^{3+}, as also evidenced by the 694 nm feature in the visible absorption spectrum of the pink axinite. This result is not surprising, even though no Cr was detected in our chemical analysis: only trace amounts of chromium are needed to yield a distinct red luminescence. In fact, luminescence is one of the most sensitive techniques available to detect this element, even at very low concentrations (e.g. <1 ppm in solids; Gaft *et al.* 2005).

According to Jobbins *et al.* (1975), the presence of vanadium could reduce luminescence intensity in axinite, and this was verified in a blue colour-zoned crystal (Arlabosse *et al.* 2008). It is possible that V^{3+} could absorb some of the Mn^{2+} emission. However, our blue sample 3356 did not show less fluorescence than the axinites of other colours (i.e. without V).

DISCUSSION

The results obtained for the average RI measurements, optic character and SG values of our samples are consistent with data listed in the gemmological literature for axinite (Liddicoat 1987; O'Donoghue 2006; Association Française de Gemmologie 2013).

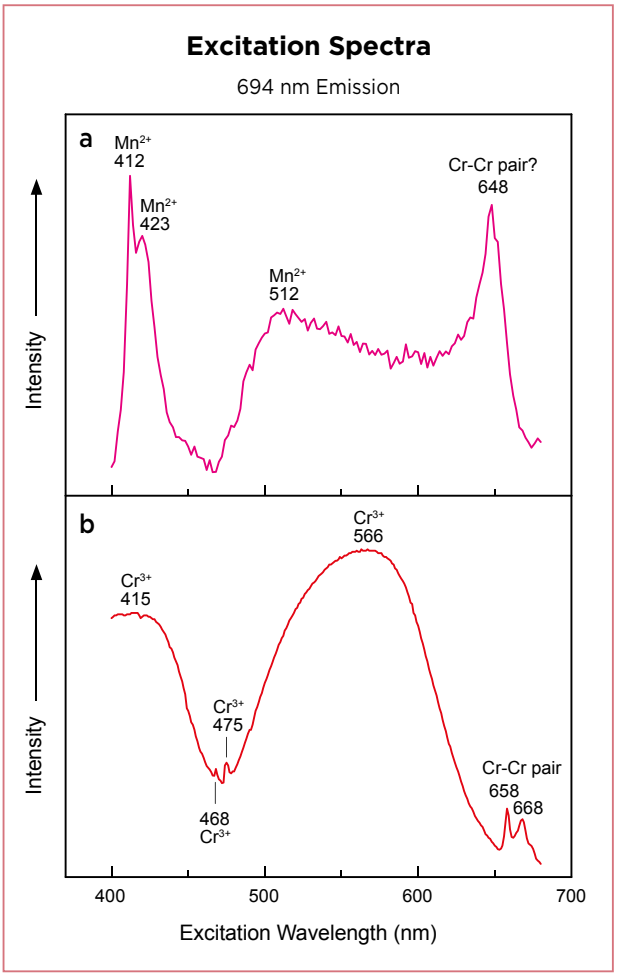

Figure 12: (**a**) The excitation spectrum of axinite sample 3000 for 694 nm emission is also related to Mn^{2+} absorption (cf. Figure 11), but shows an additional band at about 648 nm along with underlying, broad absorption in the 550–650 nm region. (**b**) Evidence of these features—ascribed to Cr-Cr ion pairs—is seen in the excitation spectrum of ruby for 694 nm emission.

Our Raman spectroscopy results for axinite-(Fe) were consistent with the detailed work of Frost *et al.* (2007). Although Raman spectroscopy cannot help assess origin of colour or luminescence, the spectra did reveal correlations with the three different axinite species represented by our specimens, providing support and confirmation of their identification based on chemical composition alone. A comparison of the reference spectra for the three axinite species in the RRUFF database also shows some consistent small differences in band positions, possibly due to variations in their chemical composition. Further work is needed to assess the exact Raman spectral band positions for the three axinite species in order for this technique to be helpful for gem identification. Relatively pure representatives of the different axinite end members, especially axinite-(Mn) and axinite-(Mg), should be carefully documented, in particular to establish the characteristic peak positions as they relate to composition. In addition, obtaining spectra from oriented samples would be helpful for evaluating the influence of crystal orientation on the relative intensity of the various bands.

We propose that Mn^{3+} is responsible for the pink colour of axinite. Ideally, it would have been preferable to obtain crystallographically oriented, polarised absorption spectra to further support our proposition. However, pink axinites are extremely rare and our samples were not transparent, so such spectra could not be obtained at this point. Another possible avenue of research would be to synthesise colourless Mn^{2+}-bearing axinite and then try irradiating it to obtain pink colouration due to Mn^{3+}.

At the Merelani deposit, the presence of some manganese as Mn^{3+} could be explained by prolonged exposure to nearby naturally occurring radioactive elements. One such source could be U impurities in zircon (Malisa 2005; Feneyrol 2012). In addition, Malisa (2003) detected higher-than-normal levels of U in igneous and sedimentary rocks in this area (although metamorphic units such as the graphite gneiss host rock were not mentioned). A third source of natural radioactivity could be K-bearing minerals present at Merelani, such as the fuchsite variety of muscovite and K-feldspar in the surrounding gneisses. Reinitz and Rossman (1988) showed that pink-to-red tourmaline from granitic pegmatites could be naturally irradiated by gamma rays from ^{40}K in the surrounding K-feldspar. At Merelani, the appearance of the pink colour would be expected to occur during retrograde metamorphism since the higher temperatures attained during peak prograde metamorphism (up to 691°C; Feneyrol 2012) would destroy the pink colour.

CONCLUSION

We conclude that the colouration of the two pink Tanzanian axinites studied for this report results from Mn^{3+} absorption. This colouring agent is likely due to natural irradiation of a small portion of Mn^{2+} that is abundant in this deposit. The UV luminescence of axinite is due to two cations: Mn^{2+} and Cr^{3+}. The first induces the dominant orange colour and the second contributes red. The weak cat's-eye effect in one cabochon examined in this study is mostly due to a combination of parallel, reflective fractures (cleavages?) and the elongated high-domed cabochon cut. While characterising our samples with Raman spectroscopy, it became apparent that more work is needed to firmly establish the Raman spectral characteristics of axinite-(Mn), axinite-(Mg) and axinite-(Fe).

REFERENCES

Arlabosse, J.-M., Rondeau, B. & Fritsch, E. 2008. Gem News International: A blue manganaxinite. *Gems & Gemology*, **44**(1), 81.

Association Française de Gemmologie 2013. *Gemmes*. Association Française de Gemmologie, Paris, France, 268 pp.

Burke, E.A.J. 2008. Tidying up mineral names: An IMA-CNMNC scheme for suffixes, hyphens and diacritical marks. *Mineralogical Record*, **39**(2), 131–135.

Burns, R.G. 1993. *Mineralogical Applications of Crystal Field Theory*, 2nd edn. Cambridge University Press, Cambridge, 551 pp., https://doi.org/10.1017/CBO9780511524899.

El Ali, A., Barbin, V., Calas, G., Cervelle, B., Ramseyer, K. & Bouroulec, J. 1993. Mn^{2+}-activated luminescence in dolomite, calcite and magnesite: Quantitative determination of manganese and site distribution by EPR and CL spectroscopy. *Chemical Geology*, **104**(1–4), 189–202, https://doi.org/10.1016/0009-2541(93)90150-h.

Faye, G.H. 1972. Relationship between crystal-field splitting parameter, "Δ_{VI}", and M_{host}–O bond distance as an aid in the interpretation of absorption spectra of Fe^{2+}-bearing materials. *Canadian Mineralogist*, **11**(2), 473–487.

Feneyrol, J. 2012. *Pétrologie, géochimie et genèse des gisements de tsavorite associées aux gneiss et roches calco-silicatées graphiteux de Lemshuku et Namalulu, Tanzanie*. Doctorat de l'Institut National Polytechnique de Lorraine spécialité Géosciences Thesis, University of Lorraine, France, 885 pp., https://hal.univ-lorraine.fr/tel-01750042/document.

Fritsch, E. & Waychunas, G. 1994. Gemstones. *In*: Robbins, M. (ed) *Fluorescence: Gems and Minerals Under Ultraviolet Light*. Geoscience Press, Phoenix, Arizona, USA, 149–174.

Fritz, E.A., McClure, S.F., Shen, A.H., Laurs, B.M., Simmons, W.B. & Falster, A.U. 2007. Gem News International: Color-zoned axinite from Pakistan. *Gems & Gemology*, **43**(3), 254–255.

Frost, R.L., Bouzaid, J.M., Martens, W.N. & Reddy, B.J. 2007. Raman spectroscopy of the borosilicate mineral ferroaxinite. *Journal of Raman Spectroscopy*, **38**(2), 135–141, https://doi.org/10.1002/jrs.1574.

Gaft, M., Reisfeld, R. & Panczer, G. 2005. *Modern Luminescence Spectroscopy of Minerals and Materials*. Springer-Verlag, Berlin, Germany, 356 pp., https://doi.org/10.1007/978-3-319-24765-6.

Gribble, C.D. & Hall, A.J. 1992. *Optical Mineralogy: Principles and Practice*. Chapman & Hall, New York, New York, USA, 303 pp., https://doi.org/10.1007/978-1-4615-9692-9.

Harris, C., Hlongwane, W., Gule, N. & Scheepers, R. 2014. Origin of tanzanite and associated gemstone mineralization at Merelani, Tanzania. *South African Journal of Geology*, **117**(1), 15–30, https://doi.org/10.2113/gssajg.117.1.15.

Jang-Green, H., Beaton, D., Laurs, B.M., Simmons, W.B. & Falster, A.U. 2007. Gem News International: Two axinite species from Tanzania. *Gems & Gemology*, **43**(4), 373–375.

Jaszczak, J.A. & Trinchillo, D. 2013. Miracle at Merelani – A remarkable occurrence of graphite, diopside, and associated minerals from the Karo mine, Block D, Merelani Hills, Arusha region, Tanzania. *Rocks & Minerals*, **88**(2), 154–165, https://doi.org/10.1080/00357529.2013.763671.

Jobbins, E.A., Tresham, A.E. & Young, B.R. 1975. Magnesioaxinite, a new mineral found as a blue gemstone from Tanzania. *Journal of Gemmology*, **14**(8), 368–375, https://doi.org/10.15506/JoG.1975.14.8.368.

Lauf, R.J. 2007. Collector's guide to the axinite group. *Rocks & Minerals*, **82**(3), 216–220, https://doi.org/10.3200/rmin.82.3.216-221.

Liddicoat, R.T. 1987. *Handbook of Gem Identification*, 12th edn. Gemological Institute of America, Santa Monica, California, USA, 362 pp.

Malisa, E.P.J. 2003. Trace elements characterization of the hydrothermally deposited tanzanite and green grossular in the Merelani–Lelatema shear zone, northeastern Tanzania. *Tanzania Journal of Science*, **29**(1), 45–60, https://doi.org/10.4314/tjs.v29i1.18366.

Malisa, E.P. 2005. Petrography and mineral chemistry of the pelitic and semi-pelitic gneisses of the Merelani tanzanite mining area, northeastern Tanzania. *Tanzania Journal of Science*, **31**(2), 81–92, https://doi.org/10.4314/tjs.v31i2.18423.

Malisa, E. & Muhongo, S. 1990. Tectonic setting of gemstone mineralization in the Proterozoic metamorphic terrane of the Mozambique Belt in Tanzania. *Precambrian Research*, **46**(1–2), 167–176, https://doi.org/10.1016/0301-9268(90)90071-w.

Milton, C., Hildebrand, F.A. & Sherwood A.M. 1953. The identity of tinzenite with manganoan axinite. *American Mineralogist*, **38**(11–12), 1148–1158.

O'Donoghue, M. (ed) 2006. *Gems*, 6th edn. Butterworth-Heinemann, Oxford, 873 pp.

Olivier, B. 2006. *The geology and petrology of the Merelani tanzanite deposit, NE Tanzania*. PhD thesis, University of Stellenbosch, South Africa, 434 pp., https://pdfs.semanticscholar.org/94ba/83d0808bc85df942494d1052a5729c903611.pdf.

Pay, D. 2017. Gem News International: Magnesio-axinite from Merelani, Tanzania. *Gems & Gemology*, **53**(1), 128–129.

Platonov, A.N., Taran, M.N. & Klyakhin, V.A. 1989. On two colour types of Mn^{3+}-bearing beryls. *Zeitschrift*

der Deutschen Gemmologischen Gesellschaft, **38**(4), 147–154.

Pohl, D., Guillemette, R., Shigley, J. & Dunning, G.E. 1982. Ferroaxinite from New Melones Lake, Calaveras County, California, a remarkable new locality. *Mineralogical Record*, **13**(5), 293–302.

Quinn, E.P. & Breeding, C.M. 2005. Lab Notes: Yellowish orange magnesioaxinite. *Gems & Gemology*, **41**(2), 170–171.

Reinitz, I.M. & Rossman, G.R. 1988. Role of natural radiation in tourmaline coloration. *American Mineralogist*, **73**(7–8), 822–825.

Robbins, M. 1994. *Fluorescence: Gems and Minerals Under Ultraviolet Light*. Geoscience Press, Phoenix, Arizona, USA, 384 pp.

Schmetzer, K. 1982. Absorptionsspektroskopie und Farbe von V^{3+}-haltigen natürlichen Oxiden und Silikaten – ein Beitrag zur Kristallchemie des Vanadiums. *Neues Jahrbuch für Mineralogie, Abhandlungen*, **144**(1), 73–106, https://doi.org/10.1127/njma/144/1982/73.

Williams, C., Williams, B. & Laurs, B.M. 2014. Gem Notes: Colour-change axinite-(Mn) from Tanzania. *Journal of Gemmology*, **34**(3), 191–192.

Wilson, W.E., Saul, J.M., Pardieu, V. & Hughes, R.W. 2009. Famous mineral localities: The Merelani tanzanite mines, Lelatema Mountains, Arusha region, Tanzania. *Mineralogical Record*, **40**(5), 346–408.

The Authors

Maxence Vigier* and Dr Emmanuel Fritsch FGA
Institut des Matériaux Jean Rouxel, CNRS and University of Nantes, UMR6502, BP32229, F-44322 Nantes Cedex 3, France
Email: Emmanuel.Fritsch@cnrs-imn.fr
* Mr Vigier was a BS student at the time of this research.

Acknowledgements

Dudley Blauwet (Dudley Blauwet Gems, Louisville, Colorado, USA) loaned sample 2999 for an extended period for research. We also thank Joyce van Dronkelaar-Kessy (Kilimanjaro Gemstones, Oostburg, the Netherlands) and Denis Gravier (Gravier & Gemmes, L'Abergement-de-Varey, Jura, France) for providing samples for this study. Prof. Edward Grew (University of Maine, Orono, Maine, USA) considerably improved the original text through a very constructive review. Laurent Lenta (Laboratoire de Planétologie et Géodynamique de Nantes, University of Nantes and CNRS) helped with sample preparation. Féodor Blumentritt (IMN-CNRS, Nantes) provided a helpful review of the manuscript. For Figure 1, we thank Vance Gems for loaning the samples and Dr Jaroslav Hyršl for providing the UV lamp used to take the luminescence image. Melli Rose (University of Arizona, Tucson, Arizona, USA) confirmed the identification of some of the samples in Figure 1 as axinite by Raman analysis.

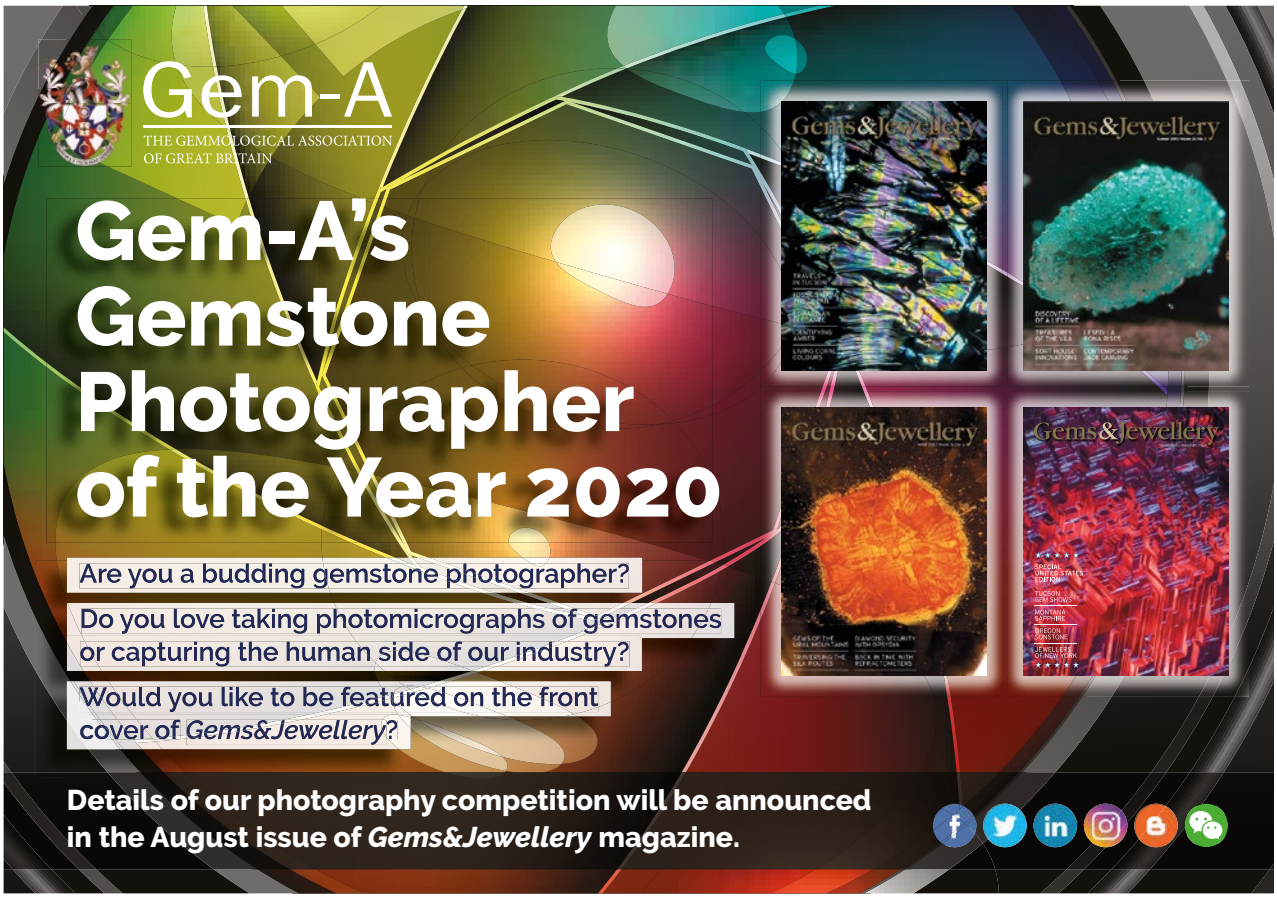

View publication stats